

# New Local Volume Dwarf Galaxy Candidates from the DESI Legacy Imaging Surveys

I. D. Karachentsev<sup>1,\*</sup> E. I. Kaisina<sup>1</sup>

<sup>1</sup>*Special Astrophysical Observatory, Russian Academy of Sciences, Nizhnii Arkhyz, 369167 Russia*

We undertook a search for new dwarf galaxies in the vicinity of relatively isolated nearby galaxies with distances  $D < 12$  Mpc and stellar masses in the  $(2 \times 10^{11} - 3 \times 10^8 M_{\odot})$  interval, using the data from the DESI Legacy Imaging Surveys. Around the 46 considered Local Volume galaxies, 67 new candidates for satellites of these galaxies were found. About half of them are classified as spheroidal dwarfs of low surface brightness. The new galaxies are included in the Local Volume database (LVGDB), which now contains 1421 objects, being 63% more than the Updated Nearby Galaxy Catalog.

Keywords: galaxies: dwarf—galaxies: groups: general—surveys

## 1. INTRODUCTION

Numerical modeling of the large scale structure of the Universe carried out by various international teams within the framework of the standard cosmological model  $\Lambda$ CDM (Klypin et al. 1999, 2016, Moore et al. 1999, Sawala et al. 2016, Tinker et al. 2010) needs comparing with the observational data on galaxies that are contained in a fixed volume of space. However, most existing catalogs comprise samples limited by the apparent magnitude (flux) of the galaxies in one spectral region or another. The first attempt to create a catalog of galaxies located within a 10 Mpc radius sphere around us was undertaken by Kraan-Korteweg and Tammann (1979). That sample contained 179 galaxies with radial velocities  $V_{LG} < 500 \text{ km s}^{-1}$  relative to the Local Group (LG) centroid. Systematic searches for nearby dwarf galaxies over the all sky (Karachentsev et al. 2000, Karachentseva and Karachentsev 1998, Karachentseva et al. 1999) in the photographic prints of the Palomar survey (POSS-II, ESO-SERC) and subsequent measurements of their radial velocities (Huchtmeier et al. 2001, 2003, 2000) led to a significant increase of the Local Volume (LV) galaxy sample. The Catalog of Neighboring Galaxies (CNG) contained 450 galaxies with expected distances  $D < 10$  Mpc (Karachentsev et al. 2004). Mass spectral surveys of large areas of the sky in the optical region: 2dF (Colless et al. 2003),

6dF (Jones et al. 2009), SDSS (Abazajian et al. 2009) and in the HI 21 cm radio line: HIPASS (Doyle et al. 2005); ALFALFA (Haynes et al. 2018) have significantly enriched the Local Volume sample. Over nine years, the number of galaxies with  $D < 10$  Mpc has almost doubled. The Updated Nearby Galaxy Catalog (UNGC) now contained 869 objects (Karachentsev et al. 2013).

Various data on LV galaxies were collected in the LVG database<sup>1</sup> (Kaisina et al. 2012), which is regularly updated with new objects. To date, this sample contains 1250 LV galaxy candidates with  $D < 11$  Mpc distances. Evidently, the new additions are mainly due to the dwarf galaxies with low integral luminosity and low surface brightness.

We should note that a significant part of the galaxies in the LVG database are merely candidates for this sample. Nearby galaxies may have radial velocities that differ significantly from the ideal Hubble velocity  $V_{LG} = H_0 D$ , where  $H_0$  is the Hubble parameter, due to the virial motions in nearby groups and large scale flows. Thus, some LV galaxies take part in a systematic flow towards the closest massive attractor in the Virgo cluster as well as in the motions away from the center of the expanding Local Void. The amplitude of both these flows reaches about  $200 \text{ km s}^{-1}$  (Tully et al. 2008), which is comparable to the quantity  $V_{LG} < 600 \text{ km s}^{-1}$  used to include galaxies in the LV.

\*Electronic address: idkarach@gmail.com

<sup>1</sup> <http://www.sao.ru/lv/lvgdb>

Great progress in the LV sample formation was reached due to mass distance measurements for galaxies based on the Hubble Space Telescope (HST) data. Using the tip of the red giant branch (TRGB) luminosity as a distance indicator allows one to determine the distance to galaxies of any morphological type with an accuracy of about 5%. HST observations with the ACS camera in the *F814W* and *F606W* filters make it possible to measure the galaxy distances by the TRGB method up to the LV boundary ( $D \sim 11$  Mpc) over a single orbital period. A list of TRGB-distance estimates for approximately 450 LV galaxies was compiled by Anand et al. (2021) and is available in the Extragalactic Distance Database (EDD)<sup>2</sup>. Obviously, high precision galaxy distance measurements lead both to an increase of the LV sample and to an exclusion of part of the objects from the nearby galaxy candidates.

In addition to the surveys of large areas of the northern and southern sky, a noticeable contribution to the LV galaxy sample additions is due to the searches for dwarf galaxies around nearby massive Milky Way (MW) and M31 (Andromeda) type galaxies. The entourage of galaxies accompanying the dominating Local Group galaxies, MW and M31, already amounts to about 50 members each (Kashibadze and Karachentsev 2018, Putman et al. 2021). Chiboucas et al. (2013, 2009) carried out a search for new dwarf galaxies in the vicinity of the neighboring M81 galaxy using long-exposure frames obtained with the CFHT telescope for subarcsecond images. These images enabled the estimation of the TRGB position for dwarfs and thus to verify their group membership. A similar approach was then used to search for new satellites around NGC 5128 (Cen A), NGC 253, NGC 628, NGC 4631, NGC 4736 (Crnojević et al. 2019, Davis et al. 2021, Müller et al. 2019, Mutlu-Pakdil et al. 2022, Okamoto et al. 2019, Smercina et al. 2018, Tanaka et al. 2017, Trujillo et al. 2021) using the CFHT and other large telescopes (Subaru, VLT, GMT, LBT, Blanco) mounted in locations with good astroclimate and equipped

with wide-field CCD-cameras. Usually, the authors aimed to carry out surveys in areas limited by the virial radius of the massive “host” galaxy. For MW and M31, the virial radius of the dark halo is  $R_{\text{vir}} \sim 250$  kpc. CCD-images taken with hours-long exposures using amateur small-aperture telescopes (Javanmardi et al. 2016, Karachentsev et al. 2020, Martínez-Delgado et al. 2021) have also made a noticeable contribution to the detection of nearby dwarf galaxy candidates.

The DESI Legacy Imaging Surveys (Dey et al. 2019), covering wide regions in the northern and southern sky, served as a significant stimulus to search for dwarf galaxies of low surface brightness. It is a combination of three projects: the Dark Energy Camera Legacy Survey, the Beijing-Arizona Sky Survey, and the Mayall z-band Legacy Survey. As of January 2021, this survey (DR9) covers a sky area of about 14 000 square degrees at galactic latitudes  $|b| > 18^\circ$ . Carried out in three optical bands,  $g$ ,  $r$  and  $z$ , this survey has a median  $5\sigma$ -limit of  $r \simeq 23.^m1$  for galaxies with an exponential profile and effective radius  $0''.5$ , which is approximately  $1^m$  deeper than the SDSS survey. Carlsten et al. (2022) used the DESI Legacy Imaging Surveys in combination with archival images obtained with the CFHT to search for satellites around massive MW-type LV galaxies. Besides the already known satellites, the authors found 68 new LV candidate members. They used the surface brightness fluctuation method (sbf) (the main contribution to which is due to the individually unresolvable red giant branch stars) to obtain new distance estimates for 130 dwarf galaxies. This outstanding paper also contains  $g$ - and  $r$ -band photometry results for over 300 Local Volume galaxies. We included the new data from Carlsten et al. (2022) in the LVG database.

## 2. SEARCH FOR NEW DWARF GALAXIES

The list of detected satellite candidates for 25 nearby massive galaxies (Carlsten et al. 2022) has about 400 objects. More than 80% of them were already included in our database of LV galaxies. The total area of the virial zones where

<sup>2</sup> <http://edd.ifa.hawaii.edu>

Carlsten et al. (2022) searched for new satellites amounts to 280 square degrees or 2% of the total area covered by the DESI Legacy Imaging Surveys. Evidently, the remaining large area may contain other new candidate LV members. An inspection of the entire remaining region of the DESI Legacy Imaging Surveys is a rather difficult task. We therefore restricted our search to dwarf satellites around the relatively isolated nearby galaxies, less massive than the MW. We used the list of LV galaxies with known satellites (Karachentsev and Kashibadze 2021) as a reference point.

The list of “host” galaxies around which we searched for new satellites includes 46 galaxies and is presented in Table 1. The following quantities are given in its columns: (1)—

name of the galaxy; (2)—equatorial coordinates in degrees for the J 2000.0 epoch; (3) and (4)—distance to the galaxy in Mpc and the method used to determine it: TRGB—the tip of the red giant branch, SN—supernovae luminosity, sbf—surface brightness fluctuations, TF—Tully-Fisher relation; NAM—radial velocity with allowance for the peculiar velocity field in the Numerical Action Method model, Shaya et al. (2017); (5)—logarithm of the  $K_s$ -band luminosity of the galaxy; (6) and (7)—angular and linear projected distance that limited the search area for the galaxy satellite candidates. Data on the galaxy distances and  $K$ -band luminosities were taken from our updated LV galaxy database, LVGDB, which also contains the data source references.

**Table 1:** List of survey regions around central galaxies

Galaxy	RA (J 2000) Dec, deg	$D$ , Mpc	Method	$\log L_K, L_\odot$	$r_p$ , deg	$R_p$ , kpc
(1)	(2)	(3)	(4)	(5)	(6)	(7)
NGC 628	24.174 +15.783	10.19	TRGB	10.60	2.3	410
NGC 672	26.977 +27.433	7.18	TRGB	9.65	2.0	250
UGC 1281	27.382 +32.588	5.27	TRGB	8.57	0.5	50
NGC 784	30.321 +28.837	5.37	TRGB	8.67	1.6	150
NGC 855	33.515 +27.877	9.73	sbf	9.37	1.2	205
NGC 1744	74.991 -26.022	10.00	TF	9.42	1.1	190
NGC 2337	107.556 +44.457	11.86	TRGB	9.34	0.8	165
NGC 2366	112.223 +69.212	3.28	TRGB	8.70	1.1	65
NGC 2403	114.202 +65.603	3.19	TRGB	9.86	2.7	150
NGC 2683	133.172 +33.421	9.82	TRGB	10.81	1.8	310
NGC 2787	139.828 +69.203	7.48	sbf	10.19	2.1	280*
NGC 2903	143.042 +21.502	9.17	TRGB	10.85	1.9	305
M 81	148.888 +69.065	3.70	TRGB	10.95	6.2	400
NGC 3184	154.570 +41.424	11.12	SN	10.52	2.3	450
NGC 3239	156.276 +17.162	10.17	SN	9.74	1.2	210
NGC 3344	160.880 +24.922	9.82	TRGB	10.33	1.5	255
NGC 3432	163.130 +36.619	9.14	TRGB	9.64	1.4	220

**Table 1:** (Continued)

Galaxy	RA (J2000) Dec, deg	$D$ , Mpc	Method	$\log L_K, L_\odot$	$r_p$ , deg	$R_p$ , kpc
(1)	(2)	(3)	(4)	(5)	(6)	(7)
NGC 3556	167.879 +55.674	9.90	TF	10.52	1.5	260
NGC 3627	170.062 +12.992	11.12	TRGB	11.08	3.0	570
NGC 3990	179.398 +55.459	10.30	sbf	9.52	1.1	200*
NGC 4136	182.324 +29.927	6.67	NAM	9.24	1.3	150*
NGC 4144	182.494 +46.457	6.89	TRGB	9.25	1.3	155
NGC 4204	183.808 +20.659	7.01	NAM	9.12	1.1	140
NGC 4236	184.176 +69.463	4.41	TRGB	9.61	2.1	160
NGC 4242	184.376 +45.619	7.62	TRGB	9.47	1.1	150
NGC 4244	184.374 +37.807	4.31	TRGB	9.52	2.0	150
NGC 4395	186.454 +33.547	4.76	TRGB	9.47	1.8	150
NGC 4449	187.048 +44.090	4.27	TRGB	9.68	2.0	150
NGC 4460	187.190 +44.864	7.28	NAM	9.66	1.2	155
NGC 4490	187.651 +41.644	8.91	TRGB	10.28	2.0	310
NGC 4517	188.190 +00.115	8.36	TRGB	10.27	1.7	250
NGC 4559	188.990 +27.960	8.91	TRGB	10.20	1.7	265
NGC 4592	189.827 -00.532	9.08	TRGB	9.16	0.7	110
NGC 4594	189.998 -11.623	9.55	TRGB	11.32	3.2	525*
NGC 4597	190.054 -05.797	10.10	TF	9.48	0.6	105
NGC 4600	190.096 +03.118	9.29	TRGB	9.33	0.6	100
NGC 4605	189.997 +61.609	5.55	TRGB	9.70	2.1	205
NGC 4618	190.387 +41.151	7.66	TRGB	9.62	1.5	200
NGC 4631	190.533 +32.542	7.35	TRGB	10.49	2.4	305
NGC 4736	192.721 +41.120	4.41	TRGB	10.56	5.3	410
NGC 4861	194.760 +34.859	9.95	TRGB	9.13	1.2	205
NGC 5023	198.052 +44.041	6.05	TRGB	9.01	1.2	125
NGC 5055	198.954 +42.030	9.04	TRGB	11.00	2.9	455
NGC 5194	202.469 +47.195	8.40	SN	10.97	3.1	450
NGC 6503	267.360 +70.144	6.25	TRGB	10.00	1.8	200

**Table 1:** (Continued)

Galaxy	RA (J2000) Dec, deg	$D$ , Mpc	Method	$\log L_K, L_\odot$	$r_p$ , deg	$R_p$ , kpc
(1)	(2)	(3)	(4)	(5)	(6)	(7)
IC 5201	335.239 -46.036	10.40	TF	10.15	1.3	235

According to Tully (2015), the virial radius  $R_{\text{vir}}$  and total mass of the galaxy halo  $M_T$  are connected by an empirical relation

$$(R_{\text{vir}}/215 \text{ kpc}) = (M_T/10^{12} M_\odot)^{1/3}.$$

The total galaxy  $K$ -band luminosity is often used to estimate  $M_T$ , assuming  $M_T/L_K \sim (20\text{--}30)M_\odot/L_\odot$ . However, this relation varies noticeably as a function of stellar mass, as well as the galaxy morphological type (Karachentsev et al. 2022, Kourkchi and Tully 2017). The choice of  $R_{\text{vir}}$  and  $R_p$  is therefore rather subjective.

The surroundings of 11 massive MW type galaxies presented in Table 1 were investigated by Carlsten et al. (2022). We have repeated the search for dwarf galaxies of low surface brightness with the survey zone expanded beyond the virial radius. Strictly speaking, a search for satellites should be carried out within the limits of the zero velocity sphere radius  $R_0$ , where the gravitational influence of the “host” galaxy dominates over the general cosmological expansion. However, for a typical ratio  $R_0/R_{\text{vir}} \simeq 3.5$ , the searching task becomes ten times harder.

Four galaxies in Table 1 are marked by an asterisk. For some reason or other, the distance estimates obtained for them may not match the real values. The distance estimate (7.48 Mpc) for NGC 2787 made by surface brightness fluctuations is not reliable. There are also indirect indications that this galaxy may be located at  $D \sim 12$  Mpc. Another, more distant, galaxy NGC 3998 near NGC 3990 is located at 14.2 Mpc (sbf). The retinues of both galaxies are practically indistinguishable from each other. The NGC 4136 galaxy is located in a region of a specific scattered group Coma I around NGC 4150, where galaxies with velocities  $V_{\text{LG}} \sim (100\text{--}300) \text{ km s}^{-1}$  have distances of about 15 Mpc. For the NGC 4594 (Sombrero)

galaxy, the southern boarder of DESI Legacy Imaging Surveys passes through the declination of  $-8^\circ 5'$ , and therefore our search for satellites covers only a small part of this galaxy’s virial zone.

Note also that the results of our search for new dwarf galaxies around the neighbor galaxies NGC 3115 and NGC 3521 were reported earlier (Karachentsev et al. 2022). The rich group around NGC 3379 has a virial radius noticeably larger than 300 kpc, the value used to search for dwarfs in Carlsten et al. (2022). We suggest revisiting the survey of this group’s surroundings later.

Our searches for possible satellites around 46 LV galaxies led to the discovery of 67 dwarf galaxies. Their images taken from the DESI Legacy Imaging Surveys catalog are presented in the form of a mosaic in the Appendix. The size of each image corresponds to  $120''$ , the north is at the top, the east is to the left.

The data on the new candidates in the LV are presented in the columns of Table 2: (1)—galaxy name; (2)—equatorial coordinates (J2000.0); (3)—maximally visible angular diameter of the galaxy in minutes of arc, approximately corresponding to the Holmberg isophote; (4)—apparent axial ratio; (5)—total  $B$ -band apparent magnitude; for relatively bright galaxies, the  $B$  values are taken from LEDA and NED, and for fainter galaxies the apparent magnitude was estimated by comparison with other galaxies of similar structure with  $g$ - and  $r$ -magnitudes measured by Carlsten et al. (2022); the relation  $B = g + 0.313(g - r) + 0.227$  was used to determine  $B$ , proposed by Lupton (see <http://www.sdss3.org/dr10/algorithms/sdssUBVRITransform.php/>); the accuracy of our visual estimations of  $B$  amounts to about  $0^m 25$ ; (6)—morphological type of the galaxy determined by us: Sph—spheroidal,

Irr—irregular, Tr—transition type between Sph and Irr, BCD—blue compact dwarf, dE—dwarf elliptical galaxy; galaxies of high (H), normal (N), low (L) and very low (VL) surface brightness are marked by the specified letters; based on the photometry results for similar objects (Carlsten et al. 2022), we estimated that the central  $r$ -band surface brightness of our galaxies lies in the (22.5–26.5) mag/sq.arcsec

range; (7)—distance to the galaxy in Mpc; (8)—method used to estimate the distance: mem—by the assumed membership in the entourage of the host galaxy; TF or bTF—by the usual or baryonic Tully-Fisher relation, NAM—by the radial velocity with allowance for peculiar velocities due to local flows; sbf—by the surface brightness fluctuations; txt—a rough distance estimate by the texture of the galaxy.

**Table 2:** New candidate LV galaxies from the DESI Legacy Imaging Surveys

Name	RA (J2000) Dec	$a_{\text{Ho}}$ , arcmin	$b/a$	$B_T$ , mag	Type	$D$ , Mpc	Method
(1)	(2)	(3)	(4)	(5)	(6)	(7)	(8)
Dw 0143+1338	01 43 55.2 +13 38 42	0.86	0.86	18.6	Sph-VL	12.3	mem
Dw 0149+3237	01 49 50.9 +32 37 42	0.40	0.95	21.5	Sph-VL	5.3	mem
Dw 0158+3018	01 58 54.7 +30 18 50	0.67	0.40	18.4	Tr-L	5.4	mem
Dw 0214+2836	02 14 09.6 +28 36 47	0.44	0.48	19.0	Irr-L	9.7	mem
Dw 0218+2813	02 18 04.1 +28 13 01	0.72	0.91	21.3	Sph-VL	9.7	mem
[KKS 2000]05	02 49 26.1 -13 12 42	1.02	0.43	17.3	Irr-L	10.0	txt
Dw 0827+6452	08 27 16.3 +64 52 26	0.45	0.87	20.5	Sph-L	3.7	mem
PGC 025409	09 02 50.6 +71 18 22	1.16	0.73	16.3	BCD-N	7.5	mem
Dw 0910+7326	09 10 15.6 +73 26 24	2.35	0.88	17.0	Sph-L	3.7	mem
Dw 0910+6942	09 10 42.1 +69 42 11	0.37	0.82	19.1	Sph-L	7.5	mem
Dw 0916+6944	09 16 43.7 +69 44 01	0.57	0.33	19.3	Irr-L	7.5	mem
Dw 0918+6935	09 18 34.9 +69 35 43	0.27	0.85	20.0	Sph-L	7.5	mem
Dw 0919+6932	09 19 07.8 +69 32 54	0.30	0.62	20.1	Tr-L	7.5	mem
UGC 4918	09 19 17.7 +69 48 04	1.00	0.53	16.0	Im-N	7.5	mem
Dw 0919+6955	09 19 33.9 +69 55 20	0.42	0.65	19.5	Sph-L	7.5	mem
Dw 0920+6924	09 20 02.6 +69 24 45	0.18	0.80	20.4	Sph-L	7.5	mem
Dw 0920+7017	09 20 22.4 +70 17 29	0.48	0.51	19.3	Sph-L	7.5	mem
Dw 0927+6818	09 27 27.8 +68 18 55	0.53	0.76	19.6	Irr-L	7.5	mem
Dw 1012+4259	10 12 42.7 +42 59 31	0.62	0.75	19.0	Tr-N	11.1	mem
Dw 1051+6416	10 51 16.1 +64 16 41	0.33	0.93	21.0	Sph-L	9.0	txt
Dw 1051+3617	10 51 27.6 +36 17 10	0.28	0.73	20.5	Sph-L	9.1	mem



**Table 2:** (Continued)

Name	RA (J2000) Dec	$a_{\text{Ho}}$ , arcmin	$b/a$	$B_T$ , mag	Type	$D$ , Mpc	Method
(1)	(2)	(3)	(4)	(5)	(6)	(7)	(8)
KDG 74	11 02 21.8 +70 15 50	0.85	0.67	18.6	Sph-L	3.7	mem
Dw 1108+5520	11 08 59.5 +55 20 28	0.33	0.80	19.5	Sph-L	9.9	mem
Dw 1109+5447	11 09 13.2 +54 47 10	0.34	0.78	19.7	Irr-L	9.9	mem
Dw 1111+1338	11 11 35.0 +13 38 38	0.32	0.90	20.5	Sph-L	11.1	mem
Dw 1113+5541	11 13 10.1 +55 41 17	0.42	0.64	20.5	Tr-L	9.9	mem
Dw 1119+1011	11 19 30.7 +10 11 56	0.46	0.65	18.1	BCD-H	11.1	mem
Dw 1127+1346	11 27 13.0 +13 46 52	0.35	0.92	20.1	Sph-L	11.1	mem
UGC 6451	11 28 46.4 +79 36 07	2.66	0.53	16.5	Im-N	3.7	mem
Dw 1159+5554	11 59 56.6 +55 54 54	1.50	0.60	19.7	Tr-L	10.3	mem
[KK 98] 121	12 05 24.5 +43 42 28	0.86	0.79	15.17	Sph-L	10.0	txt
Dw 1214+2101	12 14 18.2 +21 01 08	0.30	0.67	20.1	Sph-L	7.0	mem
Dw 1214+2945	12 14 26.6 +29 45 50	1.02	0.45	17.3	Tr-N	6.7	mem
Dw 1215+2041	12 15 32.2 +20 41 00	0.40	0.71	18.7	Tr-L	7.0	mem
Dw 1224+3938	12 24 34.6 +39 38 10	0.48	0.77	19.0	Tr-L	8.9	mem
Dw 1229+4109	12 29 43.2 +41 09 43	0.29	0.60	19.3	Sph-L	8.9	mem
Dw 1234+4116	12 34 38.2 +41 16 34	0.54	0.81	17.2	BCD-H	8.45	NAM
KDG 162	12 35 01.6 +58 23 08	1.04	0.69	18.5	Irr-L	10.0	txt
Dw 1235+7050	12 35 59.5 +70 50 53	0.60	0.57	19.0	Irr-L	4.4	mem
Dw 1237+3304	12 37 02.2 +33 04 59	0.50	0.60	17.5	Sph-N	10.90	sbf
Dw 1238+3337	12 38 18.0 +33 37 59	0.60	0.92	17.2	Tr-N	11.57	sbf
AGC 724993	12 38 30.0 +29 03 18	0.61	0.87	17.1	Im-N	9.20	TF
Dw 1239+2827	12 39 13.4 +28 27 14	0.55	0.59	18.7	Sph-L	8.9	mem
Dw 1240+3037	12 40 39.8 +30 37 55	0.40	0.83	20.1	Sph-VL	7.35	mem
Dw 1241+4103	12 41 01.0 +41 03 11	0.33	0.76	19.1	Tr-L	7.7	mem
Dw 1241-0427	12 41 22.3 -04 27 50	0.83	0.90	19.7	Sph-VL	10.1	mem
KDG 187	12 42 17.8 +03 28 08	1.35	0.93	15.6	dE-N	9.3	mem
[KK 98] 162	12 45 26.8 +18 18 01	1.12	0.64	17.7	Tr-L	10.0	txt
Dw 1245+6158	12 45 49.0 +61 58 08	0.81	0.49	18.4	Tr-L	5.6	mem

**Table 2:** (Continued)

Name	RA (J2000) Dec	$a_{\text{Ho}}$ , arcmin	$b/a$	$B_T$ , mag	Type	$D$ , Mpc	Method
(1)	(2)	(3)	(4)	(5)	(6)	(7)	(8)
Dw 1247–0824	12 47 25.0 –08 24 29	1.71	0.66	15.5	BCD–N	9.55	mem
Dw 1248–0915	12 48 38.4 –09 15 22	0.76	0.77	17.4	Sph–L	9.55	mem
EVCC 2232	12 50 04.7 –00 13 57	0.61	0.82	19.2	Sph–L	6.01	NAM
Dw 1252–0904	12 52 03.4 –09 04 26	0.34	0.70	19.5	Irr–L	9.55	mem
AGC 221126	12 56 18.0 +34 39 25	1.44	0.85	16.71	Im–N	9.5	bTF
[KK 98] 175	12 59 01.0 +35 28 48	0.77	0.72	17.51	Irr–N	9.9	mem
Dw 1311+4051	13 11 41.3 +40 51 47	0.37	0.61	19.1	Irr–N	9.0	mem
Dw 1311+4317	13 11 45.6 +43 17 06	0.75	0.84	19.2	Sph–VL	9.0	mem
Dw 1315+4304	13 15 00.5 +43 04 55	1.46	0.94	19.4	Sph–VL	9.0	mem
[KK 98] 206	13 33 22.8 +49 06 07	1.03	0.66	14.87	Im–N	9.31	TF
Dw 2215–4528	22 15 25.4 –45 28 37	0.38	0.92	19.2	Sph–L	10.4	mem
Dw 2216–4539	22 16 07.4 –45 39 11	1.08	0.71	17.5	Sph–L	10.4	mem
Dw 2217–4633	22 17 32.4 –46 33 50	0.44	0.83	18.5	Sph–L	10.4	mem
6dF J22	22 18 48.7 –46 13 05	0.53	0.50	16.1	Im–N	10.4	mem
Dw 2221–4608	22 21 03.4 –46 08 02	1.03	0.90	20.1	Irr–VL	10.4	mem
ESO 289–020	22 21 11.5 –45 40 34	1.56	0.22	15.8	Sd	10.4	mem
Dw 2221–4607	22 21 43.2 –46 07 01	0.35	0.53	20.4	Tr–VL	10.4	mem
Dw 2227–4623	22 27 06.7 –46 23 10	0.51	0.83	16.8	Tr–N	10.4	mem

Out of the 67 LV candidate dwarf galaxies that we found, 50 are not represented in the LEDA (Makarov et al. 2014) and NED<sup>3</sup> databases. Some of the brightest galaxies from Table 2 are mentioned in the SDSS, GALEX (Bianchi et al. 2017) or WISE<sup>4</sup> surveys, but are not marked as possible nearby objects.

<sup>3</sup> <http://ipac.caltech.edu>

<sup>4</sup> <http://wise2.ipac.caltech.edu/docs/release/allsky/>

### 3. REMARKS ON INDIVIDUAL CASES

*Dw0143+1338.* This very low surface brightness galaxy falls in our survey region around NGC 628. However, it is located at 13' to the east of the peculiar galaxy NGC 660, the distance to which is 12.3 Mpc (NAM), and is probably a satellite of NGC 660 rather than NGC 628.

*Dw 0149+3237.* A very low surface brightness galaxy marked by Annibali et al. (2020).

*Dw 0910+7326.* The galaxy is partially resolved into stars. It is extraordinary that it was not detected earlier.

*UGC 6451.* In contact with a distant galaxy UGC 6450, whose radial velocity is



14500 km s<sup>-1</sup>.

*Dw 1159+5554*. The object is located in the vicinity of an S0-galaxy NGC 3390. Has an unusual form of a smooth “bean” without signs of star formation. The nature of this object is mysterious.

*Dw 1214+2945*. This dwarf galaxy has a radial velocity of  $V_{LG} = 395$  km s<sup>-1</sup> (SDSS). As is the case with its neighbor spiral NGC 4136, it is located in the region of the Coma I group, where galaxies at distances of about 15 Mpc have high negative peculiar velocities.

*Dw 1234+4116*. A blue dwarf galaxy with a radial velocity of  $V_{LG} = 640$  km s<sup>-1</sup> (SDSS), probable satellite of NGC 4618 with  $V_{LG} = 576$  km s<sup>-1</sup>.

*Dw 1237+3304* and *Dw 1238+3337*. According to the distance measurements for these galaxies in Carlsten et al. (2022), both dwarf galaxies are located behind the NGC 4631 group.

*AGC 724993*. The radial velocity of this galaxy,  $V_{LG} = 736$  km s<sup>-1</sup> (Haynes et al. 2018), and its TF-distance, 9.2 Mpc, indicate that it belongs to the satellites of NGC 4559 ( $V_{LG} = 576$  km s<sup>-1</sup> and TRGB-distance 8.91 Mpc).

*KDG 187*. This is VCC 1917 with radial velocity  $V_h = 731$  km s<sup>-1</sup>, a possible Virgo cluster member.

*Dw1247-0824*. An HI-signal with a radial velocity of  $V_h = 1215$  km s<sup>-1</sup> is noticeable in HIPASS at the location of this BCD dwarf.

*EVCC 2232*. A possible Virgo cluster member with a radial velocity of  $V_{LG} = 608$  km s<sup>-1</sup> or a dwarf in front of the cluster.

*AGC 221126=UGCA 309*. A gas-rich dwarf with radial velocity  $V_{LG} = 747$  km s<sup>-1</sup> in the vicinity of NGC 4861.

*[KK 98]175=AGC 223250*. Another possible NGC 4861 satellite with a radial velocity of  $V_{LG} = 725$  km s<sup>-1</sup>. It had earlier been assigned an erroneous radial velocity of  $V_{LG} = 1205$  km s<sup>-1</sup>.

*Dw1315+4304*. A spheroidal dwarf galaxy of very low surface brightness, separated from NGC 5055 by a projected distance 175 kpc.

*[KK 98]206*. This is the blue dwarf galaxy SBS 1331+493 with radial velocity  $V_h = 594$  km s<sup>-1</sup>, a possible distance satellite of

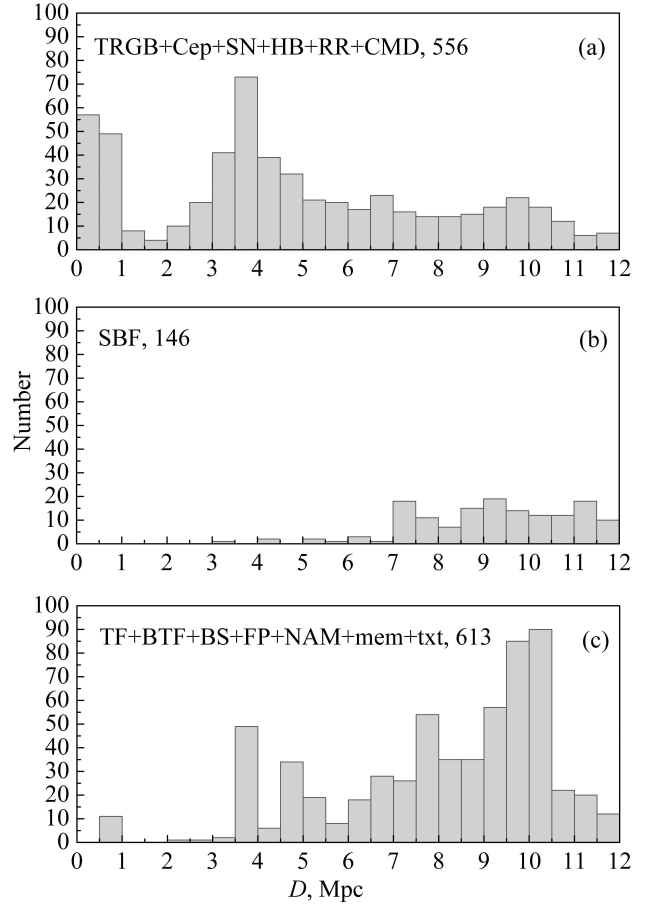


**Figure 1:** Distribution of Local Volume galaxies by distance  $D$ , estimated using methods with various accuracies: approximately 5%, 15% and 25%—panels (a), (b) and (c), correspondingly.

M 51.

*6dF J 22 and ESO 289-020*. Satellites of an Scd-galaxy IC 5201. Their heliocentric radial velocities, 996 km s<sup>-1</sup> and 917 km s<sup>-1</sup>, were measured by Kleiner et al. (2019).

#### 4. DISCUSSION

In order to confirm the status of the Local Volume members, one needs radial velocity and distance measurements for the presented candidates. The most promising method would be to determine the distances by TRGB luminosity with HST or by surface brightness fluctuations using images obtained with large ground-based telescopes with subarcsecond seeing. The more

“test particles” (dwarf galaxies) with known peculiar velocities are contained in the LV, the more accurately can the 3D-contour of the dark matter in the Local Volume be reconstructed. Such a task is currently unachievable in the more distant volumes of the Universe.

The galaxy distribution in the LV by distance from the Milky Way is presented in Fig. 1. Fig. 1a shows 499 galaxies with  $D$  estimated by the TRGB method, the accuracy of which is about 5%. To these galaxies we added another 57 with distances measured by the supernovae luminosity (SN), Cepheids (cep), RR Lyrae type stars (RR), horizontal branch (HB) and CMD galaxies (CMD). Fig. 1b corresponds to the subsample of galaxies with distances estimated by the surface brightness fluctuations ( $N = 146$ ). The  $D$  measurement accuracy for them is about 15%. Fig. 1c presents the remaining LV galaxies with distances estimated by the Tully–Fisher method (TF, BTF,  $N = 174$ ), by the radial velocity in the NAM model ( $N = 81$ ), by the assumed membership in groups (mem,  $N = 329$ ), by the brightest stars (BS,  $N = 10$ ), and also by the general texture of the galaxies (txt,  $N = 19$ ). The averaged accuracy of the distances estimated using these methods can be adopted as approximately equal to 25%. Fig. 1 does not show the 106 galaxies whose distances turned out to be greater than 12 Mpc.

Evidently, galaxies with accurately measured distances dominate in a 6 Mpc radius sphere. Near the far boundary of the Local Volume, most galaxies have distances measured with a low accuracy. On the whole, the relative number of LV galaxies with reliably measured distances does not yet exceed 40%. Curiously, in 2001, by the start of systematic TRGB distance measurements with the HST, the number of known LV galaxies was about 450. Over the past 22 years this method was used to measure TRGB-distances for approximately 500 LV galaxies, but the LV population itself became three times larger over this time. (The wolf will follow the rabbit, but will probably never catch it).

Currently, radial velocities are measured for 893 galaxies with distances within 12 Mpc. Fig. 2 shows the behavior of the Hubble flow

in the Local Volume for three types of galaxies shown in Fig. 1. A trend can be seen: the higher the distance measurement accuracy, the smaller the Hubble diagram scatter. In Fig. 2a, the typical accuracy of the galaxy distance estimates is only (0.3–0.6) Mpc, and therefore, their deviation from the ideal Hubble flow is due to their real peculiar velocities. In Fig. 2b, the Hubble diagram looks expressionless. Due to the absence of emission lines in the radio and optical spectra for the dwarf spheroidal galaxies, only a quarter of them have measured radial velocities. In some cases (dw 1240–1140), distances measured by the surface brightness fluctuations may contain significant errors.

In Fig. 2c, the main mass comprises galaxies with distances estimated by the Tully–Fisher relation between the internal motions amplitude and total galaxy luminosity. Additionally, the diagram shows 85 galaxies with kinematic NAM model distance estimates (green circles). The scatter of these galaxies with respect to the straight line characterizes the role of systematic non-Hubble flows in the Local Volume. Fig. 2c does not show seven dwarf galaxies: VCC 114, VCC 169, KDG 104, UGC 7642, VCC 1675, IC 3591 and VCC 1713. They are all located near the direction towards the Virgo cluster center, they have TF-distances between 7 and 10 Mpc and radial velocities in the interval from 1400 to 2100  $\text{km s}^{-1}$ , taking part in accelerated motion towards the cluster center. The same effect also influences the galaxies UGC 7512, Coma P and GR 34 with TRGB-distances marked in Fig. 2a.

If we exclude the members of the known nearby groups with their virial motions from Fig. 2a, the Hubble diagram for the remaining general field galaxies (with negative “tidal index”  $\Theta_1$  in the UNGC catalog) will take the form presented in Fig. 3. At small distances  $D < 2.5$  Mpc, the Hubble flow looks “cold” with a characteristic peculiar velocity of  $\sigma_v \sim 30 \text{ km s}^{-1}$ . The close galaxies at a distance of the order of 1 Mpc have decreased radial velocities due to their deceleration by the total mass of the Local Group. Large scale flows begin to manifest themselves at larger distances. The red circles in Fig. 3 show three galaxies in the di-

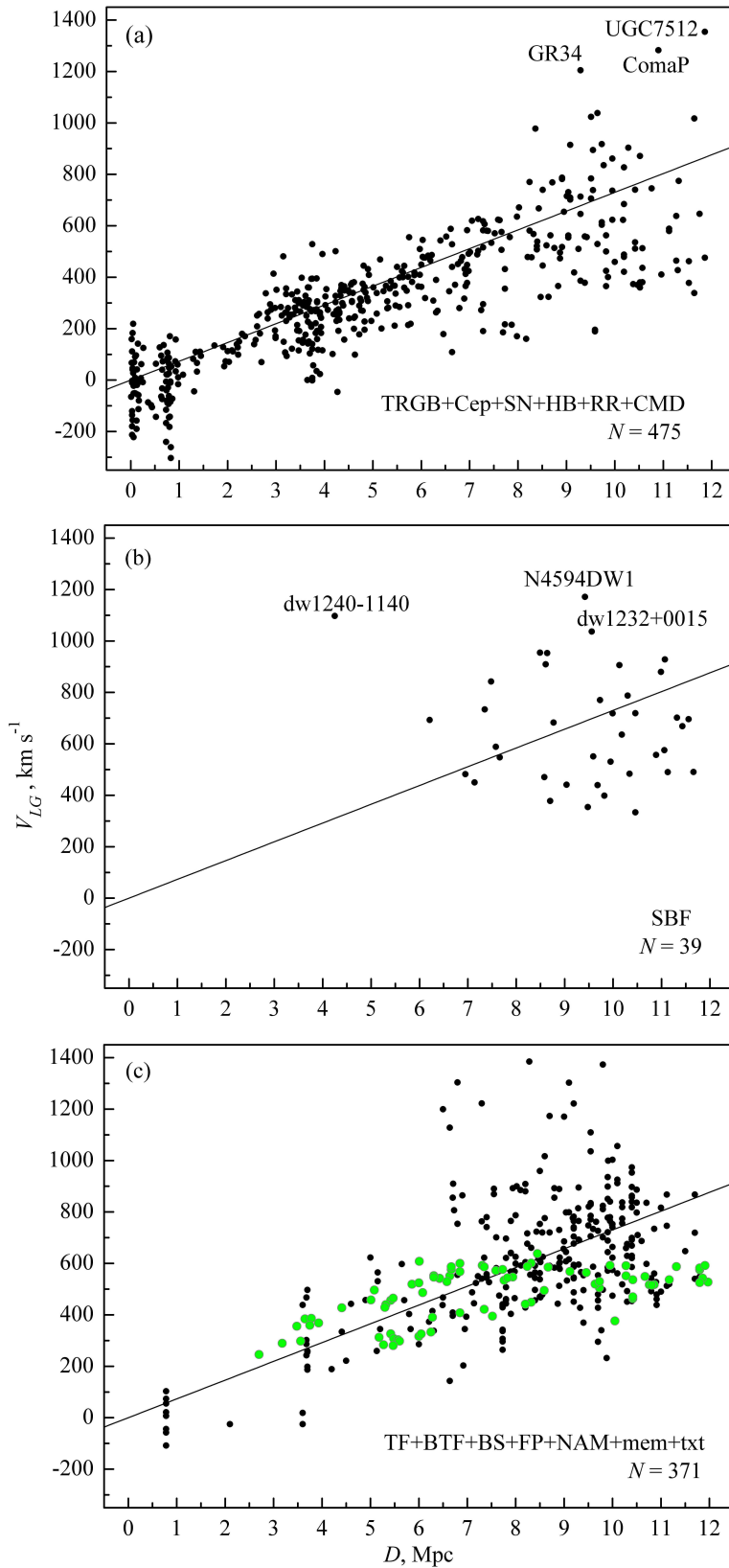


**Figure 2:** Distribution of the Local Volume galaxies by radial velocities relative to the Local Group centroid and by distance from the Milky Way. Panels (a), (b) and (c) show galaxies with high, medium and low accuracy distance estimates, correspondingly. The straight line corresponds to the Hubble parameter  $73 \text{ km s}^{-1} \text{ Mpc}^{-1}$ . In panel (c), galaxies with kinematic distance estimates (NAM) are shown by the green circles.

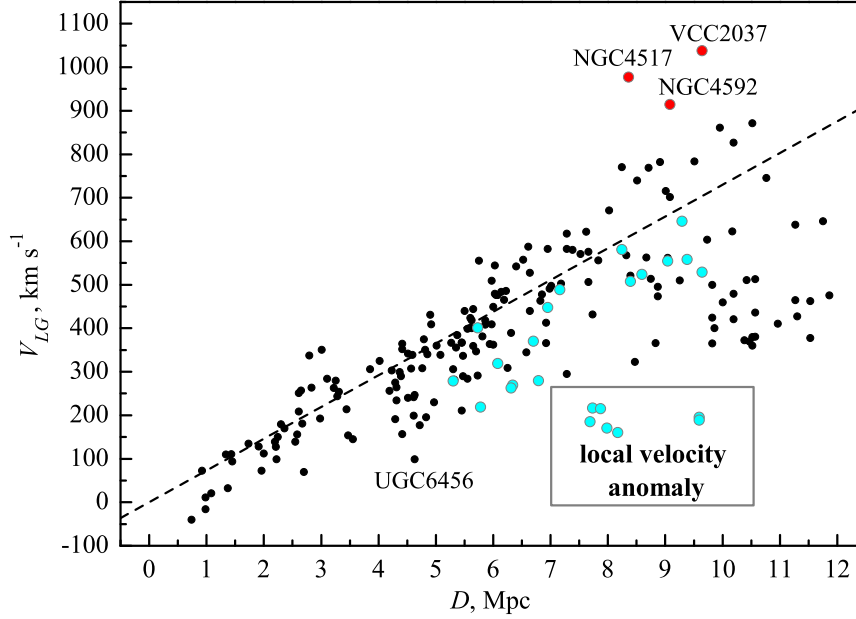


**Figure 3:** Hubble “velocity–distance” relation, similar to Fig. 2, but for the general field galaxies with negative tidal indices. Galaxies in a  $13^\circ$  radius cone around the center of the Virgo cluster are shown by the red circles, whereas galaxies at high negative supergalactic latitudes are shown by cyan circles. The straight line corresponds to the unperturbed Hubble flow with the parameter  $73 \text{ km s}^{-1} \text{ Mpc}^{-1}$ .

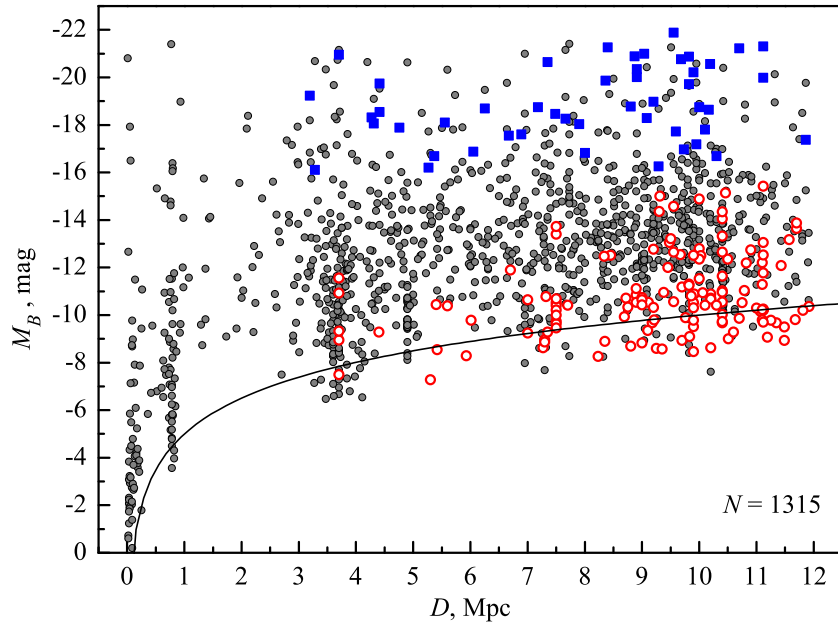


**Figure 4:** Distribution of the Local Volume galaxies by absolute  $B$ -magnitude and distance from the Milky Way. The blue squares show the galaxies around which we searched for new satellites. The open red circles show the new Local Volume candidates, recently found in the DESI Legacy Imaging Surveys. The curve corresponds to the total apparent magnitude of the galaxies  $B_t = 20^m0$ .

rection of the Virgo cluster within a  $13^\circ$  radius from its center. The cyan circles show galaxies at supergalactic latitudes  $SGB < -45^\circ$ . Seven of them, with velocities of the order of  $200 \text{ km s}^{-1}$  and distances 8–9 Mpc, are located in the zone of the so-called “local velocity anomaly”. The deviations of the first category of galaxies from the unperturbed Hubble flow with the parameter  $H_0 = 73 \text{ km s}^{-1} \text{ Mpc}^{-1}$  is due to the falling of these galaxies towards the closest massive attractor Virgo. The deviations of the second category of galaxies are caused by their systematic motion from the center of the expanding Local Void. An analysis of the local peculiar velocity field allows one to estimate the total mass of the Virgo cluster,  $M_T = 8 \times 10^{14} M_\odot$  (Karachentsev et al. 2014), as well as the size and density contrast of the Local Void (Nasonova and Karachentsev 2011). Generally, the combination of isolated nearby galaxies follows the Hubble relation with a slope of not 73, but  $60 \text{ km s}^{-1} \text{ Mpc}^{-1}$ . This is probably due to an excess of objects at high supergalactic latitudes among the nearby isolated galaxies.

The distribution of LV galaxies by absolute  $B$ -magnitudes and distances from the MW is shown in Fig. 4. The blue squares show the galaxies around which we searched for new satellites. The red empty circles mark the galaxies added to the LV sample based on our data and the data of Carlsten et al. (2022) in the process of searching in the DESI Legacy Imaging Surveys. A deficit of ultra-dwarf galaxies with absolute magnitudes fainter than  $-9^m$  remains noticeable near the far boundary of the Local Volume. This gap will obviously be filled in deeper sky surveys: Euclid (Laureijs et al. 2011), Roman Space Telescope (Spergel et al. 2015) and LSST, planned in the nearest years to come.

#### ACKNOWLEDGEMENTS

The authors are grateful to D. I. Makarov, who has repeated the computations of the tidal indices for the Local Volume galaxies with allowance for new data. This work has made use of the DESI Legacy Imaging Surveys data.

#### FUNDING

The work on updating the galaxy catalog was carried out within grant № 075-15-2022-262 (13.MNPMU.21.0003) of the Ministry of Science and Higher Education of the Russian Federation.

#### CONFLICT OF INTEREST

The authors declare no conflict of interest.

#### REFERENCES

- K. N. Abazajian, J. K. Adelman-McCarthy, M. A. Agüeros, et al., *Astrophys. J. Suppl.* **182** (2), 543 (2009).
- G. S. Anand, L. Rizzi, R. B. Tully, et al., *Astron. J.* **162** (2), id. 80 (2021).
- F. Annibali, G. Beccari, M. Bellazzini, et al., *Monthly Notices Royal Astron. Soc.* **491** (4), 5101 (2020).
- L. Bianchi, B. Shiao, and D. Thilker, *Astrophys. J. Suppl.* **230** (2), article id. 24 (2017).
- S. G. Carlsten, J. E. Greene, R. L. Beaton, et al., arXiv e-prints astro/ph:2203.00014 (2022).
- K. Chiboucas, B. A. Jacobs, R. B. Tully, and I. D. Karachentsev, *Astron. J.* **146** (5), id. 126 (2013).
- K. Chiboucas, I. D. Karachentsev, and R. B. Tully, *Astron. J.* **137**, 3009 (2) (2009).
- M. Colless, B. A. Peterson, C. Jackson, et al., arXiv e-prints astro/ph:0306581 (2003).
- D. Crnojević, D. J. Sand, P. Bennet, et al., *Astrophys. J.* **872** (1), article id. 80 (2019).
- A. B. Davis, A. M. Nierenberg, A. H. G. Peter, et al., *Monthly Notices Royal Astron. Soc.* **500** (3), 3854 (2021).
- A. Dey, D. J. Schlegel, D. Lang, et al., *Astron. J.* **157** (5), article id. 168 (2019).
- M. T. Doyle, M. J. Drinkwater, D. J. Rohde, et al., *Monthly Notices Royal Astron. Soc.* **361** (1), 34 (2005).
- M. P. Haynes, R. Giovanelli, B. R. Kent, et al., *Astrophys. J.* **861** (1), article id. 49 (2018).
- W. K. Huchtmeier, I. D. Karachentsev, and V. E. Karachentseva, *Astron. and Astrophys.* **377**, 801 (2001).
- W. K. Huchtmeier, I. D. Karachentsev, and V. E. Karachentseva, *Astron. and Astrophys.* **401**, 483 (2003).
- W. K. Huchtmeier, I. D. Karachentsev, V. E. Karachentseva, and M. Ehle, *Astron. and Astrophys. Suppl.* **141**, 469 (2000).

- B. Javanmardi, D. Martínez-Delgado, P. Kroupa, et al., *Astron. and Astrophys.* **588**, id. A89 (2016).
- D. H. Jones, M. A. Read, W. Saunders, et al., *Monthly Notices Royal Astron. Soc.* **399** (2), 683 (2009).
- E. I. Kaisina, D. I. Makarov, I. D. Karachentsev, and S. S. Kaisin, *Astrophysical Bulletin* **67** (1), 115 (2012).
- I. Karachentsev and O. Kashibadze, *Astronomische Nachrichten* **342** (7–8), 999 (2021).
- I. D. Karachentsev, V. E. Karachentseva, W. K. Huchtmeier, and D. I. Makarov, *Astron. J.* **127** (4), 2031 (2004).
- I. D. Karachentsev, V. E. Karachentseva, A. A. Suchkov, and E. K. Grebel, *Astron. and Astrophys. Suppl.* **145**, 415 (2000).
- I. D. Karachentsev, D. I. Makarov, and E. I. Kaisina, *Astron. J.* **145** (4), id. 101 (2013).
- I. D. Karachentsev, L. N. Makarova, G. S. Anand, and R. B. Tully, *Astron. J.* **163** (5), id. 234 (2022).
- I. D. Karachentsev, F. Neyer, R. Späni, and T. Zilch, *Astronomische Nachrichten* **341** (10), 1037 (2020).
- I. D. Karachentsev, R. B. Tully, P.-F. Wu, et al., *Astrophys. J.* **782** (4), id. 4 (2014).
- V. E. Karachentseva and I. D. Karachentsev, *Astron. and Astrophys. Suppl.* **127**, 409 (1998).
- V. E. Karachentseva, I. D. Karachentsev, and G. M. Richter, *Astron. and Astrophys. Suppl.* **135**, 221 (1999).
- O. G. Kashibadze and I. D. Karachentsev, *Astron. and Astrophys.* **609**, id. A11 (2018).
- D. Kleiner, B. S. Koribalski, P. Serra, et al., *Monthly Notices Royal Astron. Soc.* **488** (4), 5352 (2019).
- A. Klypin, A. V. Kravtsov, O. Valenzuela, and F. Prada, *Astrophys. J.* **522** (1), 82 (1999).
- A. Klypin, G. Yepes, S. Gottlöber, et al., *Monthly Notices Royal Astron. Soc.* **457** (4), 4340 (2016).
- E. Kourkchi and R. B. Tully, *Astrophys. J.* **843** (1), id. 16 (2017).
- R. C. Kraan-Korteweg and G. A. Tammann, *Astronomische Nachrichten* **300**, 181 (1979).
- R. Laureijs, J. Amiaux, S. Arduini, et al., arXiv e-prints astro/ph:1110.3193 (2011).
- D. Makarov, P. Prugniel, N. Terekhova, et al., *Astron. and Astrophys.* **570**, id. A13 (2014).
- D. Martínez-Delgado, D. Makarov, B. Javanmardi, et al., *Astron. and Astrophys.* **652**, id. A48 (2021).
- B. Moore, S. Ghigna, F. Governato, et al., *Astrophys. J.* **524** (1), L19 (1999).
- O. Müller, M. Rejkuba, M. S. Pawlowski, et al., *Astron. and Astrophys.* **629**, id. A18 (2019).
- B. Mutlu-Pakdil, D. J. Sand, D. Crnojević, et al., *Astrophys. J.* **926** (1), id. 77 (2022).
- O. G. Nasonova and I. D. Karachentsev, *Astrophysics* **54** (1), 1 (2011).
- S. Okamoto, N. Arimoto, A. M. N. Ferguson, et al., *Astrophys. J.* **884** (2), id. 128 (2019).
- M. E. Putman, Y. Zheng, A. M. Price-Whelan, et al., *Astrophys. J.* **913** (1), id. 53 (2021).
- T. Sawala, C. S. Frenk, A. Fattahi, et al., *Monthly Notices Royal Astron. Soc.* **457** (2), 1931 (2016).
- E. J. Shaya, R. B. Tully, Y. Hoffman, and D. Pomarède, *Astrophys. J.* **850** (2), id. 207 (2017).
- A. Smercina, E. F. Bell, P. A. Price, et al., *Astrophys. J.* **863** (2), id. 152 (2018).
- D. Spergel, N. Gehrels, C. Baltay, et al., arXiv e-prints astro/ph:1503.03757 (2015).
- M. Tanaka, M. Chiba, and Y. Komiyama, *Astrophys. J.* **842** (2), 127 (2017).
- J. L. Tinker, B. E. Robertson, A. V. Kravtsov, et al., *Astrophys. J.* **724** (2), 878 (2010).
- I. Trujillo, M. D’Onofrio, D. Zaritsky, et al., *Astron. and Astrophys.* **654**, id. A40 (2021).
- R. B. Tully, *Astron. J.* **149** (2), id. 54 (2015).
- R. B. Tully, E. J. Shaya, I. D. Karachentsev, et al., *Astrophys. J.* **686** (2), id. 1523 (2008).

*Translated by L. Chmyreva*



## APPENDIX

Images of candidate satellites for nearby massive galaxies, taken from DESI Legacy Imaging Surveys. The map size is  $2' \times 2'$ . North is at the top, east is to the left.

